View metadata, citation and similar papers at core.ac.uk

brought to you by CORE

provided by Open Research Online

Open Research Online

The Open University's repository of research publications
and other research outputs

A New Mutual Information based Similarity Measure for Medical Image Registration

Conference or Workshop Item

How to cite:

Reel, Parminder Singh; Dooley, Laurence S. and Wong, Patrick (2012). A New Mutual Information based Similarity Measure for Medical Image Registration. In: IET Image Processing Conference 2012, 3-4 Jul 2012, London.

For guidance on citations see FAQs.

© 2012 IET

Version: Accepted Manuscript

Link(s) to article on publisher's website:
http://conferences.theiet.org/ipr/abstract/index.cfm

Copyright and Moral Rights for the articles on this site are retained by the individual authors and/or other copyright owners. For more information on Open Research Online's data policy on reuse of materials please consult the policies page.

oro.open.ac.uk

A NEW MUTUAL INFORMATION BASED SIMILARITY MEASURE FOR MEDICAL IMAGE REGISTRATION

Parminder Singh Reel, Laurence S. Dooley and K. C. P. Wong

Department of Communication and Systems, The Open University, Milton Keynes, United Kingdom
Email: p.s.reel|l.s.dooley|k.c.p.wong@open.ac.uk

Keywords: Medical Image Registration, Mutual Information, Principal Component Analysis.

Abstract

Medical *image registration* (IR) is the systematic process of aligning spate images, often involving different modalities with common reference framework, so complementary information can be combined and compared. This paper presents a new similarity measure which uses *Expectation Maximization* for *Principal Component Analysis* allied with *mutual information* (EMPCA-MI) for medical IR. The new measure has been analysed on multimodal, three band *magnetic resonance images* (MRI) T1, T2 and PD weighted, in the presence of both intensity non-uniformities (INU) and noise. Both quantitative and qualitative experimental results clearly demonstrate both improved robustness and lower computational complexity of the new EMPCA-MI paradigm compared with existing MI-based similarity measures, for various MRI test datasets.

1 Introduction

Magnetic resonance imaging (MRI) is one of the principal medical imaging techniques [13] for the visualisations of soft tissues in the body. Using a combination of radio and magnetic waves, MRI is available in three bands: T1, T2 and PD-weighted images. T1 (spin-lattice relaxation) and T2 (spin-spin relaxation) are the respective time constants corresponding to the imaging tissues, while PD (proton density) reflects the number of hydrogen atoms in the imaging region. These images are inherently multimodal and afford complementary structural information, so it is desirable from both a diagnosis and analysis perspective, to be able to fuse them together [15].

A vital step before fusion is to register or align these MRI, since for a variety of reasons, such as patient movement or equipment calibration errors; image misalignment can occur. Since, MRI is especially prone to non-anatomic intensity variations due to radio frequency non-uniformities and static field in-homogeneity, it collectively provide a major challenge for any standard *image registration* (IR) algorithm to solve effectively. These *intensity non-uniformities* (INU) together with noise cause the corruption of tissue images which compromises image registration quality [10]. IR involves the geometric transformation of a source image, so it attains physical alignment with a reference target image. An optimization is subsequently performed using known transformations to maximise a predefined similarity measure between the source and reference images [16].

A number of similarity measures have been proposed for IR [16], and these can be broadly classified according to whether they are based on cross-correlation, *mutual information* (MI) or Fourier techniques, with MI being foremost in the medical imaging domain [7]. MI has its roots in information theory and exploits the statistical relationship between a source and target images [1, 12] making it suitable for multimodal registration. Whilst computationally efficient and robust against outliers, it is sensitive to interpolation artefacts and when the overlap region between images is small. Normalized MI (NMI) [11] was specifically designed to solve this overlap limitation and can successfully align even partial images, provided there is some overlap with the reference image.

MI and NMI, both fail to accurately register MRI containing INU and noise. To resolve this shortcoming, neighbourhood features have been incorporated with MI to secure more robust registration. The effect of INU on IR can be reduced by splitting the MRI into several regions for feature extraction. One example is regional MI (RMI) [9], which combines local pixel regions with MI. In order to calculate the entropies, RMI uses a covariance matrix instead of a high-dimensional histogram to reduce data complexity. However, as neighbourhood region grows, so does the matrix size, leading to a commensurate computational impact.

These shortcomings in MI-based techniques caused by the high dimensionality and the ensuing effect on registration quality provided the motivation to investigate a more efficient MI-based similarity measure for IR, which is both computationally fast and robust to INU and noise, particularly in MRI. *Principal Component Analysis* (PCA) [5] is a proven technique for reducing data dimensionality and has been integrated with MI (PCA-MI) and used as an IR similarity measure. This feature extraction technique however, requires the full covariance matrix be computed even if only a few components are required, and this problem is further exacerbated as the matrix dimension increases.

This paper proposes a new MI-based similarity measure which employs *Expectation Maximisation for Principal Component Analysis* (EMPCA) [8] to achieve efficient

dimensionality reduction by iteratively determining the leading principal components. EMPCA-MI computes only the first principal component as the key feature from regions of an image, as this element gives the direction of maximum variance. This significantly reduces the computational cost, with minimal corresponding impact on the registration performance compared with other MI-based similarity measures. Quantitative results for multimodal three band MRI registration confirm the efficacy of the new EMPCA-MI paradigm from both a registration error and computation time perspective.

The remainder of the paper is organised as follows: Section 2 briefly reviews the basic principles of medical IR, MI and EMPCA, before Section 3 presents the formulation of the EMPCA-MI model. Section 4 discusses the experimental set-up and a detailed comparative results analysis for EMPCA-MI using three-band MRI test datasets. Finally, Section 5 provides some concluding comments.

2 Medical IR, MI and EMPCA

2.1 Medical IR Principles

Medical IR defines the key task of aligning a source medical image A with a target image B. As Figure 1 shows, this is a multistep and iterative process [16] which involves repeatedly: i) transforming the coordinates of the source image A with known transformation parameters T in a given reference space; ii) generating a new interpolated source image A^* in the reference space; iii) comparing A^* with the target medical image B using a similarity measure; and iv) optimising the transformation parameters T sequentially, to achieve the best possible alignment, where similarity measure value is maximum between the images. This process can be visualised as in Figure 1.

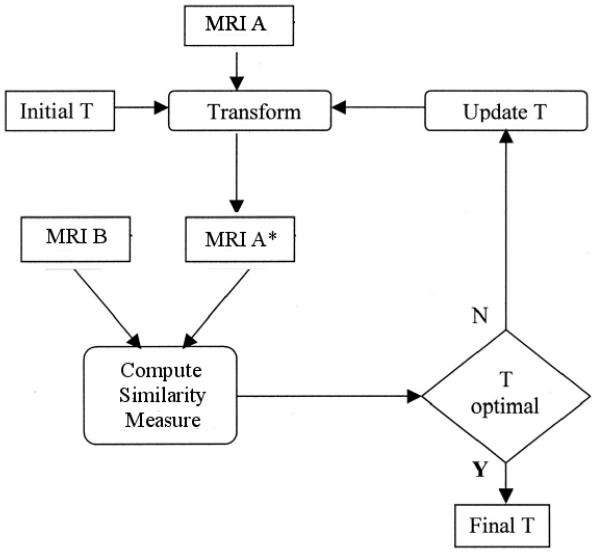

Figure 1: IR for two MRI A and B, where T is a known transformation.

2.2 MI

MI represents the amount of information one variable contains about another. It assumes a statistical relationship between them, which is reflected in their individual and joint probabilities. For MRI A and B, MI is given by:

$$I(A,B) = \sum_{a,b} p(a,b) \log\left(\frac{p(a,b)}{p(a)p(b)} \right) \qquad (1)$$

Where $p(a)$ and $p(b)$ denote the individual probabilities of A and B, while $p(a,b)$ is their corresponding joint probability. MI measures the dependence of the intensity distributions of two images. For IR, the overall objective is to maximise $I(A,B)$, so the two images are eventually aligned with minimal registration error [1, 12, 16].

2.3 EMPCA

As previously mentioned, PCA [5] has been effectively applied to extract features and formulated with MI (PCA-MI), though as with RMI, its drawback is that it is computationally intensive, especially as the size of *neighbourhood regions* (NR) is expanded. This paper uses the EMPCA [8] technique, which is an iterative process to estimate the leading principal components using an expectation and subsequent maximisation step. This avoids the requirement to compute the entire covariance matrix, making EMPCA faster than PCA. Furthermore, as the first dominant principal component provides the direction of highest variance for a given NR, it can be used for IR without significantly impacting on the overall registration accuracy. The next section introduces the EMPCA-MI model formulation, which extracts local feature information using EMPCA before applying MI to obtain the statistical relationship between the source and target MRI.

3 EMPCA-MI Similarity Measure

This section presents a new MI-based similarity measure for medical IR which is robust to both INU and noise. It combines NR information with MI using EMPCA in three constituent steps (see Figure 2). The corresponding pseudo-code for the EMPCA-MI model is given in Algorithm 1.

Step I – Pre-processing: Figure 3 graphically illustrates this step (Lines 1–4 in Algorithm 1), which involves generating the NR matrix **D** for a given pixel radius r. **D** is subsequently concatenated as a 3-dimensional matrix as it scans the whole image, ignoring the margin effects (Lines 2–4). **D** is then reshaped as the NR information matrix Q with dimensions d x N (see Figure 3 (b)) where d represents the dimensional space and N is the number of pixels scanned (Line 5). The reason for using NR is to reduce the effect of INU since intensity variations across a localised region will normally be lower than across the whole image. Since NR pixels are more likely to be locally correlated compared to pixels located further apart, each NR is rearranged as a vector, enabling features to be extracted along with dimensionality reduction by applying EMPCA. Matrix Q, is then generated for both the source and target images A and B (Line 6) as shown in Figure 3(c).

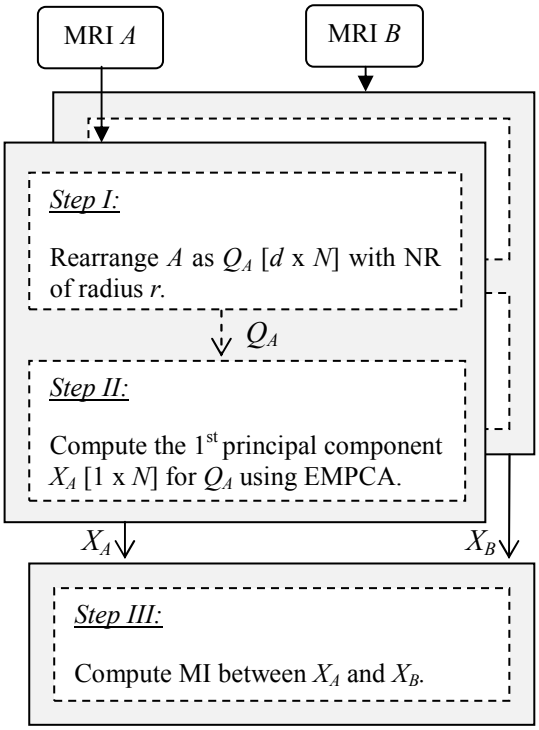

Figure 2: Key steps in the EMPCA-MI algorithm for MRI *A* and *B*

Step II – Computing EMPCA: Since conventional PCA techniques incur order $O(Nr^4)$ operations [5], the aim of this step is dimensionality reduction. By applying the iterative EM algorithm, *p* PCA components [8], where $p<d$, of the largest eigenvectors are determined to lower the computational overheads. If only the first principal component is considered for example, the complexity becomes $O(Nr^2)$ in Line 7. While there may be a corresponding performance trade-off in terms of the ensuing IR accuracy, as will be evidenced in the results in Section 4, the EMPCA-MI model experiences only minor impact in registration accuracy compared with other existing MI-based similarity measures for three-band MRI datasets.

Algorithm 1: EMPCA-MI
Inputs: MRI ***A*** and ***B*** each with spatial resolution *m* x *n* *pixels*; *r* – NR radius. **Variables:** *d*– dimensional space; *N*– total no. of pixels; *i, j, k*– indexes; **D**–NR square matrix of *size* 2*r*+1; Q_A, Q_B– NR information matrices for *A* and *B*; X_A, X_B– first principal component using EMPCA for *A* and *B* **Output:** EMPCA-MI value
1: Initialise $d = (2r+1)^2$, $N=(m-2r)(n-2r)$ and $k = 1$; 2: For *A*, $1+r \le i \le m-r$, $1+r \le j \le n-r$ 3: Define $\mathbf{D}_k=A_{([(i-r)\ldots(i+r)])([(j-r)\ldots(j+r)])}$ *4:* $k=k+1$ 5: Reshape **D** as $Q_{A([1\ldots d])([1\ldots N])}$ 6: REPEAT Steps 2 to 5 for *B* to give Q_B 7: Calculate X_A and X_B using Q_A and Q_B as in [8] 8: Calculate MI(X_A, X_B) using (1) 9: STOP

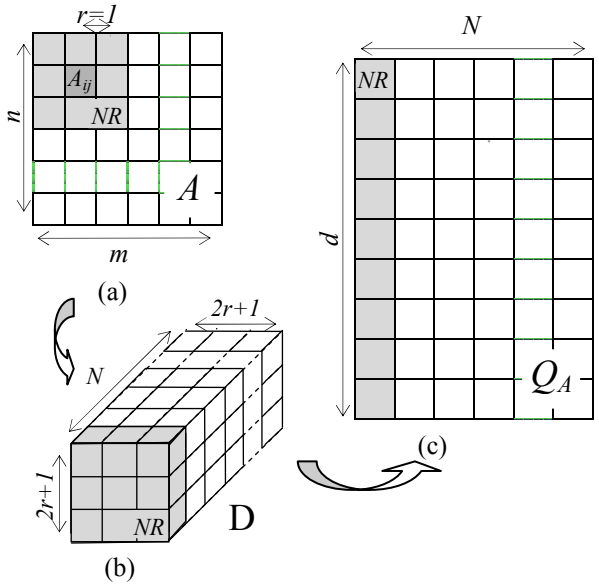

Figure 3: Illustration of EMPCA-MI Step I (a) source MRI *A* with example NR shaded (r=1) and centre pixel A_{ij}, (b) the corresponding **D** matrix, and (c) NR information matrix Q_A.

Step III – Compute MI: Once the source and target MRI are respectively arranged as *d* x *N* matrices Q_A and Q_B as illustrated in Figure 3, the corresponding principal components X_A and X_B are then extracted using EMPCA. This final step evaluates the MI between X_A and X_B using (1). EMPCA-MI only uses the first principal component as the features from regions in each MRI, because it is the direction of highest variance and thus represents the dominant features. The output value from the EMPCA-MI algorithm (Line 8) is then a measure of how closely the two MRI are aligned for the given transformation parameters.

EMPCA-MI is employed as the similarity measure in the IR process (Figure 1). IR is achieved by iteratively choosing known transformation parameters to obtain the highest EMPCA-MI value, which represents the best registration between the two MRI. While this process is computationally intensive, effective optimisation techniques are available to reduce the time complexity [16].

4 Results Discussion and Experimental Setup

A series of multimodal medical IR experiments were conducted to comparatively analyse the performance of EMPCA-MI algorithm. MRI test datasets were specially considered as they are multimodal in nature and are also a particularly challenging test scenario for EMPCA-MI in terms of INU and noise artefacts. Three dataset groups with known ground truth were created [2] (see Figure 4) for the three-band MRI i.e. T1, T2 and PD weighted image slices, with each group representing one patient. The image slices already have INU incorporated, while Gaussian noise was subsequently added to each dataset (see Table 1). The first series of experiments compared the IR performance between T1 and T2, T2 and PD, and PD and T1 MRI for the EMPCA-MI model together with two other MI-based comparative

similarity measures, namely MI and RMI. All experiments were performed upon an Ubuntu 10.04 (lucid) with 2.93 GHz Intel Core and 3GB RAM. All the assorted algorithms were implemented in MATLAB. Each experiment involved an *initial known transformation* (IKT) of predefined x and y axis translations and rotation θ as (x, y, θ). To evaluate the robustness of IR [14], five different IKT values (x_k, y_k, θ_k) were chosen, where k=2, 4, 6, 8 & 10. k=2 & 10 represent the minimum and maximum misregistration span respectively, with intermediate values being uniformly chosen to observe the robustness of IR process as the level of misregistration is increased. 540 separate IR experiments were performed, i.e., 3 groups, 3 modality-pairs, 4 INU and noise settings, 5 IKT values and 3 similarity measures.

MRI Dataset	*Resolution* (*pixels*)	*INU* (α)	*Noise* (*β*)
T1	[181x217x181]	α_{20} = 20% INU α_{40} = 40% INU	Gaussian (μ = 0.01, σ^2=0.01)
T2			
PD			

Table 1: Dataset parameter details for each of the three groups

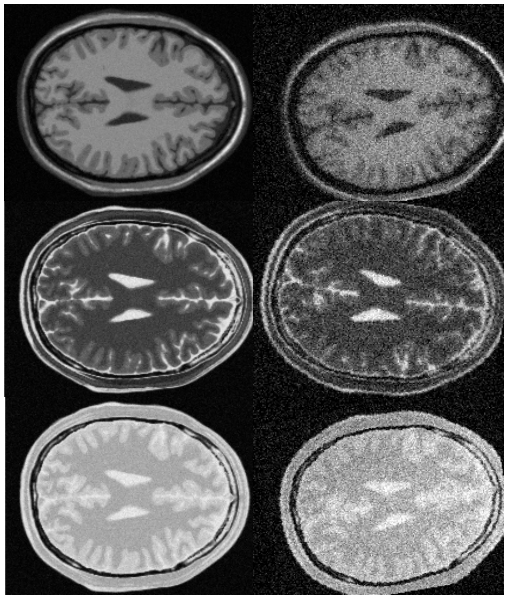

Figure 4: Sample test images: Left are the T1, T2 and PD target MRI and on the right, the corresponding source MRI including INU and Gaussian noise (see Table 1).

Exp. No	*A*	*B*		MI [1, 12]		RMI (r = 1) [9]		EMPCA-MI (r = 1)	
				ART = 0.0852secs		*ART = 0.215secs*		*ART =0.198secs*	
			IKT (x_k, y_k, θ_k)	FT (x^*, y^*, θ^*)	*RE*	FT (x^*, y^*, θ^*)	*RE*	FT (x^*, y^*, θ^*)	*RE*
1	T1	T2	k = 4	3.50, 4.50, 3.75	1.250	3.75, 4.25, 3.75	0.750	4.00, 4.25, 3.75	**0.500**
2			k = 10	8.75, 8.25, 6.50	6.500	9.50, 9.75, 7.25	3.500	9.50, 8.75, 8.50	**3.250**
3	T1+α_{20}		k = 4	3.25, 4.25, 3.50	1.500	3.25, 4.00, 3.75	1.000	3.75, 3.75, 4.50	**1.000**
4			k = 10	8.25, 7.75, 6.75	7.250	9.25, 9.25, 8.25	3.250	9.00, 8.75, 9.25	**3.000**
5	T1+α_{40}		k = 4	3.25, 3.00, 3.25	2.500	3.50, 3.25, 3.75	1.500	3.75, 3.25, 3.75	**1.250**
6			k = 10	7.50, 7.50, 6.50	8.500	9.25, 8.75, 8.50	3.500	9.00, 9.00, 8.75	**3.250**
7	T1+β		k = 4	3.25, 3.00, 3.75	2.000	3.25, 3.50, 4.00	1.250	3.50, 3.75, 4.00	**0.750**
8			k = 10	7.75, 7.50, 6.75	8.000	9.25, 9.00, 8.75	3.000	9.00, 9.25, 9.25	**2.500**
9	T1+α_{40}+β		k = 4	2.25, 2.75, 2.25	4.750	3.00, 2.75, 3.50	2.750	3.50, 3.00, 3.25	**2.250**
10			k = 10	6.75, 6.25, 5.25	11.25	9.00, 8.75, 9.00	**3.250**	9.00, 8.75, 8.75	3.500
11	T2	PD	k = 4	3.25, 2.75, 3.75	2.250	3.50, 3.75, 3.25	1.500	4.25, 4.25, 3.75	**0.750**
12			k = 10	8.00, 7.75, 6.00	8.250	8.75, 8.50, 9.00	3.750	9.25, 9.00, 9.00	**2.750**
13	T2+α_{20}		k = 4	2.50, 4.50, 4.50	2.500	4.75, 4.25, 3.25	1.750	4.50, 4.25, 3.50	**1.250**
14			k = 10	12.25, 6.50, 6.50	9.250	11.0, 8.50, 8.50	4.000	10.75, 8.25, 9.0	**3.500**
15	T2+α_{40}		k = 4	2.25, 3.75, 5.50	3.500	2.75, 3.50, 4.75	2.500	3.25, 3.25, 4.25	**1.750**
16			k = 10	12.50, 6.25, 5.75	10.25	11.75, 8.25, 8.75	4.750	11.25, 8.25, 9.25	**3.750**
17	T2+β		k = 4	2.50, 3.50, 5.25	3.250	3.75, 3.25, 4.50	1.500	3.50, 3.50, 4.25	**1.250**
18			k = 10	11.25, 7.00, 5.25	9.000	10.25, 8.25, 8.75	3.750	10.25, 8.50, 8.50	**3.250**
19	T2+α_{40}+β		k = 4	2.50, 3.75, 6.50	4.250	3.50, 8.50, 5.25	2.250	3.50, 5.25, 4.00	**1.750**
20			k = 10	12.75, 5.25, 5.00	12.50	10.75, 7.00, 8.25	5.500	10.50, 8.00, 8.50	**4.000**
21	PD	T1	k = 4	3.25, 4.50, 3.50	1.750	3.50, 4.25, 3.25	1.500	4.25, 4.00, 3.50	**0.750**
22			k = 10	7.75, 11.50, 6.25	7.500	8.75, 10.50, 8.50	3.250	9.25, 10.25, 8.75	**2.250**
23	PD+α_{20}		k = 4	3.75, 5.25, 3.25	2.250	4.00, 4.75, 3.00	1.750	4.25, 4.50, 3.25	**1.500**
24			k = 10	7.75, 11.75, 5.75	8.250	8.75, 10.75, 8.50	3.500	9.00, 10.50, 8.50	**3.000**
25	PD+α_{40}		k = 4	5.50, 4.25, 2.75	3.000	5.00, 4.00, 2.75	2.250	4.75, 4.25, 3.00	**2.000**
26			k = 10	5.75, 12.00, 6.50	9.750	8.25, 11.75, 9.25	4.250	8.75, 10.25, 8.75	**2.750**
27	PD+β		k = 4	3.50, 4.50, 2.50	2.500	3.75, 4.25, 3.25	1.250	3.50, 4.00, 3.25	**1.250**
28			k = 10	8.25, 11.00, 6.00	6.750	8.75, 10.75, 9.5	2.500	9.00, 10.5, 9.25	**2.250**
29	PD+α_{40}+β		k = 4	2.75, 5.25, 2.00	4.500	3.25, 4.75, 2.75	2.750	3.00, 4.25, 2.75	**2.500**
30			k = 10	7.75, 12.50, 5.75	9.000	8.00, 11.25, 9.50	3.750	8.25, 10.75, 8.75	**3.750**

Table 2: Registration error (RE) and average runtime (ART) results for dataset Group 1, where Exp. No is Experiment Number

The IR process uses nearest neighbour interpolation for image transformation [16], prior to applying Powell's conjugate gradient descent method [16] for optimisation. This iteratively searches the parameter space (x, y, θ) to locate the highest similarity measure value by individually maximizing each parameter. Subsequent iterations then start from maximum value found for the previous parameter. Once the maximum of all three parameters has been found, the process is repeated until a defined improvement threshold is met. This particular set of transformation parameter values is known as the *final transformation* (FT), which defines when the two MRI images are best registered. The *registration error* (RE) is calculated for each IR between IKT and FT as:

$$RE = |x - x^*| + |y - y^*| + |\theta - \theta^*| \qquad (2)$$

where (x, y, θ) and (x^*, y^*, θ^*) are the FT and IKT values respectively [14].

Table 2 displays the RE results for three-band MRI dataset (Group 1) using different INU-noise combinations and selected IKT values for MI, RMI and the new EMPCA-MI similarity measure. Since IR using IKT k=2 produce very low RE for all similarity measures, k=4 and k=10 are used for inter-experiment analysis. The corresponding *average runtimes* (ART) to compute each similarity measure are also included. For both RMI and EMPCA-MI, a NR radius of r=1 was chosen as it represented the smallest region for feature extraction. To clarify the Table 2 nomenclature, T1 represents MRI T1 slice without any INU and Gaussian noise, while T2+α_{40}+β refers to a MRI T2 image slice with both 40% INU and Gaussian noise (see Table 1). Experiment No *1, 2, 11, 12, 21 & 22* refer to three-band multimodal IR in the absence of either INU or noise. The results confirm that both RMI and EMPCA-MI consistently provided better performance than MI, with lower RE values, especially in the presence of INU and noise (see Table 2, the lowest RE values are bold). MI in contrast, only performed satisfactorily at lower IKT values in the absence of INU (Exp. No *1 & 7*). As INU levels increase and at higher IKT, the corresponding RE is significantly larger (see Exp. No *10 & 20*). Conversely for both RMI and EMPCA-MI, the IR process is able to reliably furnish lower RE values due to incorporating NR spatial information within their respective similarity measures (Exp. No *9* and *10*).

Despite using the first principal component, EMPCA-MI still achieved lower RE in the nearly all MRI combinations, while at the same time enhancing the computational efficiency (lower ART). Only in two experiments, EMPCA-MI did produce either identical RE (Exp. No *30*) or slightly higher value (Exp. No *10*) to RMI. These two scenarios were especially challenging as they involved high noise levels allied with INU, so the resulting MRI quality is substantially degraded. Since only NR of radius r=1 is used, the optimization process locks into a local maxima (giving higher RE), but this can be avoided by increasing the radius r as discussed later. Similar conclusions were drawn for the IR of the other two MRI dataset groups. To afford a complementary qualitative appreciation of EMPCA-MI, IR result of MRI *A* with FT have been overlaid with MRI *B* using the Canny edge detector [3] and a checkerboard overlaying method [4] as shown in Figure 5 for Exp. No *10.*

To quantitatively evaluate the performance of each similarity measure, the registration results were classified as either "*successful*" (RE<2.5) or "*unsuccessful*" (RE≥2.5) clinically as in [6, 9]. The graph in Figure 6 shows the percentage of successful registrations in all three MRI groups and the corresponding IKT values for the similarity measures (in the absence and presence of INU and noise). The curves provide a valuable insight into the robustness of similarity measures. In the absence of noise, all similarity measures perform well at low IKT values, but as the noise increases, both RMI and EMPCA provide superior performance compared with MI.

When IR involving both INU and Gaussian noise (α+β) is considered, it can be readily observed that all similarity measures perform well when the registration starts at IKT k=2, well justifying the use of IKT k=4 along with k=10 in Table 2. But as IKT increases, EMPCA-MI performs better than RMI and on average, has 10% more successful registrations than MI. The performance of the new EMPCA-MI model was also analysed at higher NR radii i.e., r=2 or r=3, which includes more spatial information into the similarity measure. This resolves the issue of the higher RE identified in Exp. No *10,* because the search area has now been expanded for feature extraction, and local maxima have been avoided so giving a larger global peak in the optimisation process, though there is inevitably a promotional computation cost incurred. Figure 7 illustrates misregistration performance for the EMPCA-MI model with varying r.

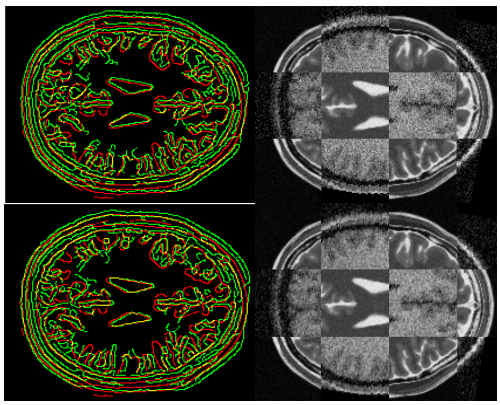

Figure 5: IR results representation for EMPCA-MI (Exp. No. *10*). The left and right images show the overlays based respectively upon Canny edges [3] and checkerboard [4], while the 1st and 2nd rows show the overlay for the ground truth and EMPCA-MI registration results.

Finally, the ART of the EMPCA-MI and RMI, for varying NR r values were evaluated for Exp. No *10*, with the corresponding results being displayed in Table 3. The times for a conventional PCA-based (PCA-MI) model [5] has also been included for comparison. Since PCA-MI generates all the eigenvectors from the covariance matrix, it has a much higher ART of 1.502*secs* compared to 0.386*secs* for EMPCA-

MI at *r=3*. It is also apparent from the results that EMPCA-MI consistently incurs a lower time overhead compared to RMI, while concomitantly affording better performance so vindicating the rationale for incorporating EMPCA in this new MI-based similarity measure.

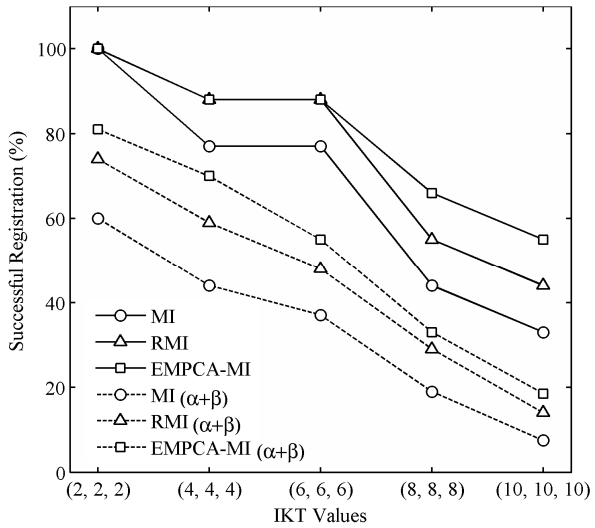

Figure 6: Overall registration robustness for various similarity measures.

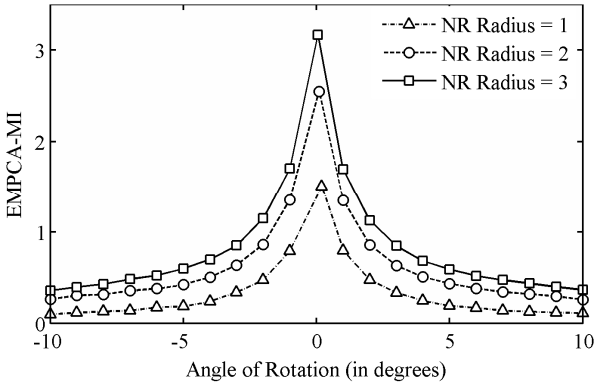

Figure 7: EMPCA-MI model misregistration performance as a function of the angle of rotation for Exp No *10.*

NR *radius*	RMI [9]	PCA-MI	EMPCA-MI
r=1	0.215	0.912	0.198
r=2	0.355	1.285	0.309
r=3	0.411	1.502	0.386

Table 3: Average runtimes (*secs*) for Exp. No *10.*

5 Conclusion

This paper has presented a new MI-based similarity measure which applies *Expectation Maximisation for Principal Component Analysis* (EMPCA-MI) to achieve more robust IR performance and enhanced computational efficiency. The EMPCA-MI model reduces the inherent dimensionality problem in other MI-based solutions, while providing analogous registration performance for various three-band medical resonance images, particularly in the presence of intensity non- uniformity and noise artefacts. The findings confirm the potential for the EMPCA-MI model to be used in other medical imaging modalities, as well as in different image domains such as remote sensing and computer vision.

References

[1] A. Collignon, F. Maes, D. Delaere, D. Vandermeulen, P. Suetens, G. Marchal, "Automated multi-modality image registration based on information theory," *Imaging*, vol. 3(1), pp. 263-274, (1995).

[2] D.L. Collins, A.P. Zijdenbos, V. Kollokian, J.G. Sled, N.J. Kabani, C.J. Holmes, A.C. Evans, "Design and Construction of a Realistic Digital Brain Phantom" *IEEE Trans. Med. Imag*., vol.17(3), p.463–468, (1998).

[3] A. Hagemann, K. Rohr, H. S. Stiehl, U. Spetzger, J. M. Gilsbach, "Biomechanical modeling of the human head for physically based, nonrigid image registration," *IEEE Trans. Med. Imag*., vol. 18(10), pp. 875–884,(1999).

[4] L. Y. Hsu, M. H. Loew, "Fully automatic 3D feature based registration of multi-modality medical images," *Image and Vision Comput.*, vol. 19, pp. 75-85, (2001).

[5] I. Jolliffe, Principal Component Analysis, 2nd ed. New York: Springer, (2002).

[6] C.R. Maurer, J.M. Fitzpatrick, M.Y. Wang, R.L. Galloway, R.J. Maciunas, G.S. Allen, "Registration of head volume images using implantable fiducial markers," *IEEE Trans. Med. Imag.,* vol.16(4), pp.447-462, (1997).

[7] J. P. W. Pluim, J. B. A Maintz, M. A. Viergever "Mutual-information-based registration of medical images: A survey", *IEEE Trans. Med. Imag.,* vol. 22(8), pp. 986-1004, (2003).

[8] S. Roweis, "EM algorithms for PCA and SPCA," in *Adv. in Neural Info. Process. Sys.*, 10, (1998).

[9] D. B. Russakoff, C. Tomasi, T. Rohlfing, C.R. Maurer, "Image similarity using mutual information of regions." in ECCV (3), pp. 596-607, (2004).

[10] A. Simmons, P. S. Tofts, G. J. Barker, S. R. Arridge, "Sources of intensity non uniformity in spin echo images at 1.5 T," *Magn. Reson. Med.*, vol. 32, pp. 121–128, (1994).

[11] C. Studholme, D.L.G. Hill, D.J. Hawkes, "An Overlap Invariant Entropy Measure of 3D Medical Image Alignment", Pattern Recognition, vol. 32(1), pp 71-86, (1999).

[12] P. Viola, W. M. Wells III, "Alignment by maximization of mutual information", Proc. 5th Int. Conf Computer Vision, pp.16-23, (1995).

[13] G.A. Wright, "Magnetic resonance imaging," *IEEE Signal Process. Mag.*, vol. 14(1), pp.56-66, (1997).

[14] X. Yang, J. Pei, W. Xie, "Maximization of Feature Potential Mutual Information in Multimodality Image Registration Using Particle Swarm Optimization," Proc. of the SPIE, Vol. 5747, pp. 1300-1309, (2005).

[15] Y. Zheng, A. S. Elmaghraby, H. Frigui, "Three-band MRI Image Fusion Utilizing the Wavelet-based Method Optimized with Two Quantitative Fusion Metrics," Proc. of the SPIE, Vol. 6144, pp. 1-12, (2006).

[16] B. Zitova, J. Flusser, "Image registration methods: A survey", *Image Vision Computer*, vol. 21(11), pp.977-1000, (2003).